Performance analysis of robust cooperative positioning based on GPS/UWB integration for connected autonomous vehicles

Performance Analysis of Robust Cooperative Positioning based on GPS/UWB Integration for Connected Autonomous Vehicles

Yang Gao[1], Hao Jing[1], Mehrdad Dianati[1], *Senior Member, IEEE*, Craig M Hancock[2], and Xiaolin Meng[3]
[1]Warwick Manufacturing Group, University of Warwick, Coventry, CV4 7AL, UK
[2]School of Architecture, Building and Civil Engineering, Loughborough University, Loughborough, LE11 3TU, UK
[3]UbiPOS UK Ltd., Nottingham, NG8 1NA, UK

The accurate position is a key requirement for autonomous vehicles. Although Global Navigation Satellite Systems (GNSS) are widely used in many applications, their performance is often disturbed, particularly in urban areas. Therefore, many studies consider multi-sensor integration and cooperative positioning (CP) approaches to provide additional degrees of freedom to address the shortcomings of GNSS. However, few studies adopted real-world datasets and internode ranging outliers within CP is left untouched, leading to unexpected challenges in practical applications. To address this, we propose a Robust Cooperative Positioning (RCP) scheme that augments the GPS with the Ultra-Wideband (UWB) system. A field experiment is conducted to generate a real-world dataset to evaluate the RCP scheme. Moreover, the analysis of the collected dataset enables us to optimise a simple but effective Robust Kalman Filter (RKF) to mitigate the influence of outlier measurements and improve the robustness of the proposed solution. Finally, a simulated dataset is derived from the real-world data to comprehensively study the performance of the proposed RCP method in urban canyon scenarios. Our results demonstrate that the proposed solution can crucially improve positioning performance when the number of visible GPS satellite is limited and is robust against various adverse effects in such environments.

Index Terms—**Cooperative Positioning, Connected and Autonomous Vehicles, V2X Systems, GPS, UWB**

I. Introduction

MODERN vehicles are becoming increasingly connected and autonomous, dubbed as CAVs, and promise to improve road safety, help reduce traffic congestion, as well as, the air pollution [1]. Accurate positioning, often by Global Navigation Satellite System (GNSS), is a key requirement for many CAV functions. However, the poor positioning performance of GNSS in urban areas (e.g., canyons) is a well-known problem due to the lack of direct Line-Of-Sight (LOS) communications and multipath errors [2]–[5], particularly in urban environments. Therefore, stand-alone GNSS is not considered to be reliable for many CAV functions that require accurate and reliable positioning in such environments.

Extensive studies have been devoted to improving vehicle positioning accuracy and reliability by augmenting GNSS information with various other means. Multi-sensor integration is one of the primary approaches to enhance positioning performance. Various sensors data in this approach are fused with GNSS data to provide more accurate and reliable position information. For example, the following solutions can be found in the literature: Radio Frequency (RF) signal-based ranging from ground stations (e.g., Locatalites, Pseudolites, Ultra-wideband UWB - Systems), optical sensor (e.g., Light Detection And Ranging -LiDAR, camera), Inertial Measurement Units (IMU), and many other alternatives as listed in [6]–[10]. Although the aforementioned solutions have demonstrated some improvements in positioning performance, each of these candidate sensors has its own disadvantages. For example, optical sensors are highly scene dependent, the accumulating error of IMUs requires frequent correction [11] and most of RF ranging systems require a clear LOS between nodes. Besides, IMU and optical sensor may not retain to be fully reliable in the absence of GNSS as well as the high cost may reduce their application for mass-market.

In addition to the multi-sensor integration approach, a promising alternative approach of improving positioning performance is to enable cooperation among vehicles and infrastructure nodes known as Cooperative Positioning (CP) [12]. This can be achieved by enabling some form of ranging among connected vehicles and Road Side Units (RSUs) as well as exchanging information via V2X systems [13]. Internode ranging can be achieved by various methods. UWB technology is of particular interest due to its high bandwidth and fine timing resolution, which gives it the ability to produce centimetre accuracy ranging [14]. A series of studies on GPS/UWB-based CP solutions have been conducted to improve the positioning performance of the GPS-standalone solution [15], [16]. It is worth noting that UWB also suffers from noise and outliers in Non-Line-of-Sight (NLOS) situations as discussed in the literature of [17], [18], although it is in a different manner and scale compared to narrowband signals. Some studies have investigated the NLOS identification and mitigation for UWB localisation in the indoor environment [19], [20]. However, very little attention has been given to mitigate the effect of UWB outlier measurements when UWB ranging is integrated within CP solutions for vehicle positioning in the outdoor environment. In a standard positioning algorithm, UWB ranging measurement is usually considered with a higher weight than GPS pseudo-range due to the high accuracy expected from UWB signals under LOS conditions, hence, these unexpected UWB outlier measurements could induce large errors to the overall result.

The above discussions motivate that GPS-based positioning performance in the urban area can be improved from two aspects: (i) increasing redundant measurement through multi-sensor integration and cooperative positioning and (ii) mitigating the effect of outlier measurement by applying robust

estimation. To this end, a Robust Cooperative Positioning (RCP) scheme, based on the tight integration between GPS code pseudo-range and UWB ranging measurement using Robust Kalman Filter (RKF), is proposed to cope with UWB outliers and improve the integrated positioning performance, even in the absence of GPS observations. A field experiment is then conducted to evaluate the RCP method. Furthermore, an extensive simulation study is carried out to comprehensively analyse the conditions when UWB measurements can augment GPS positioning. The main contributions of this paper are threefold: (i) A Robust Cooperative Positioning (RCP) scheme is proposed to provide reliable position by integrating GPS pseudo-range and UWB ranging measurements and it particularly improve the robustness of positioning solution against outlier measurements and GPS outages. (ii) A field experiment had been conducted to collect real-world data to learn realistic measurement characteristics that is used to establish a relevant measurement error and fault model to optimise the thresholds of the RKF in our algorithm. (iii) An in-depth performance analysis backed by the collected real-world dataset and a simulated dataset is performed, which allow us to comprehensively evaluate the proposed GPS/UWB integration-based CP scheme in low GPS visibility and GPS outages scenarios. The analysis demonstrates the capabilities and limitations of the proposed CP solution in various scenarios.

The rest of this paper is organised as follows. Section II reviews the related work in the literature on GPS/UWB integration positioning solutions and relevant CP solutions. Section III defines the problem that is solving in this paper and explains the algorithm formulation of the proposed RCP method. Section IV, firstly, explains the field experiment that used to collect real data for performance analysis; it then describes how the data collected from the field experiment is extended to a simulated dataset to provide a comprehensive analysis of the proposed RCP method. Finally, the key conclusions as well as potential future work are discussed in Section V.

II. Related work

The idea of GPS/UWB integration was initially proposed in [21] to enable continuous indoor-outdoor positioning. However, only loosely-coupled approaches were considered which requires that both GPS and UWB can work independently, i.e., obtaining a sufficient number of measurement input individually. By comparison, the tightly-coupled approach has the advantages that all received measurements from the individual system can be effectively fed into a single positioning algorithm, a higher positioning accuracy can also be achieved as multi-source measurements are processed simultaneously [22]. To obtain a higher accuracy, a series of studies have been conducted to investigate the GPS carrier-phase and UWB ranging measurements tightly-coupled integration for pedestrian positioning purposes [23]–[25]. Those studies applied single or multiple UWB devices as reference stations to achieve an improved ability to correctly and quickly fix integer ambiguity. In addition to the pedestrian positioning, several studies have been conducted in the context of other domains, such as ground vehicles and air vehicles. In [26], two road-side UWB reference stations were deployed to assist the subject vehicle improving the GPS float solution and ambiguity resolution compared to the GPS-only case. In [27], [28], UWB ranging measurement was tightly integrated with GPS carrier phase and IMU measurements to improve positioning performance in terms of accuracy and robustness for unmanned aerial vehicle (UAV) positioning. Although GPS carrier-phase measurement could provide a more accurate position, it requires an expensive dual-frequency GPS receiver and convergence time, i.e., a continuous period of time under the exposure of a sufficient number of visible satellites to fix integer ambiguity. Such requirements can be challenging to meet in urban environments, thus do not appear to be advantageous over more cost-effective solutions, such as the proposed solution in this study, where the consumer-grade GPS receiver and code pseudo-range measurements are used for its low cost and efficient solution.

The development of inter-vehicle ranging via V2X communications, including UWB, enables the application of CP techniques and presents a new degree of freedom in complementing GPS measurements for vehicle positioning. Accurate and robust vehicle positioning can be achieved from obtaining the location information, raw measurement and internode distances shared between vehicles and RSUs. For vehicular CP, inter-vehicle ranging can be derived from double differenced GPS pseudo-range measurements, as in [29], which are assigned with different weights based on the carrier-to-noise ratio (CNR) of the raw measurements. However, this can be impractical in urban areas as a sufficient number of satellites need to be observed by all vehicles. A CP method is proposed in [30], [31], where the GPS measurements are integrated with the Dedicated Short Range Communication (DSRC) installed on the vehicles. The Doppler shift of the DSRC carrier is used to calculate the velocity difference between vehicles. However, a minimum relative speed, i.e. 20 km/h, between vehicles is required for the Doppler shift to be detectable, which can be disabled in congested urban driving conditions. Several studies propose to use radio frequency-based ranging technique to provide internode ranging measurement to augment GPS measurement for cooperative positioning [32]–[35]. However, their methods were mainly demonstrated through simulated GPS and internode ranging measurement, without considering the practical implications. Although field experiments were conducted in [16], [36], [37] to utilise the UWB ranging measurement with GPS measurements through tight integration, the UWB nodes were placed under ideal conditions for high accuracy ranging. Therefore, the outliers of the assisting measurements were not considered. In [38], a Non-Line-of-Sight (NLOS) GNSS signal detection algorithm based on $\chi 2$ distribution detection has been proposed to enhance the robustness of the GNSS/UWB integration CP method in urban environments. Again, it only concentrates on mitigating GNSS multipath effect and leave UWB outlier mitigation untouched. In [39], the authors proposed a cooperative integrity monitoring framework based on $\chi 2$ distribution detection that considers not only faults in the GNSS measurements, but also UWB measurement biases, such as outliers. The limitation of

this work is that the UWB outlier measurements are randomly added in simulation which cannot provide practical confidence.

Although the aforementioned works propose various CP solutions for improving positioning performance, there is little work in analysing the performance of such systems using data collected from real-world experiments, which is crucial in demonstrating their performance in practical scenarios. Furthermore, very few studies were based on the real-world dataset, their negligence of the important aspect of UWB outlier measurement, which can lead to serious problems in calculating positions, has not been properly investigated and addressed by the existing studies. In one of the authors' previous works [9], UWB data was tightly-integrated with GPS and INS to perform positioning in various environments. In this work, a different dataset is collected as we remove the need for an INS, V2I communications is extended to V2X and provide an effective method to mitigate the UWB outliers observed in real-world data by using a new set of parameters in the RKF algorithm. We also present an in-depth analysis on the collected real-world GPS and UWB measurements to help understand how UWB can augment GPS positioning under different conditions and scenarios, which was not discussed in the previous work.

III. System Model and the Proposed Solution

In this section, the proposed RCP method is explained, which aims to provide a reliable and accurate positioning solution using consumer-grade GPS (in this study, the GPS is used as a representative of the GNSS constellation) and UWB device enabled by the V2X communication. The system model will be presented firstly including the assumptions made in this paper and then the formulation of the proposed RCP method is given.

A. System model

The system model considered in this paper is depicted in Figure 1. It includes a subject vehicle (SV), driving in a road segment within the coverage of a GPS reference station and enough GPS satellite coverage (the number of visible satellite

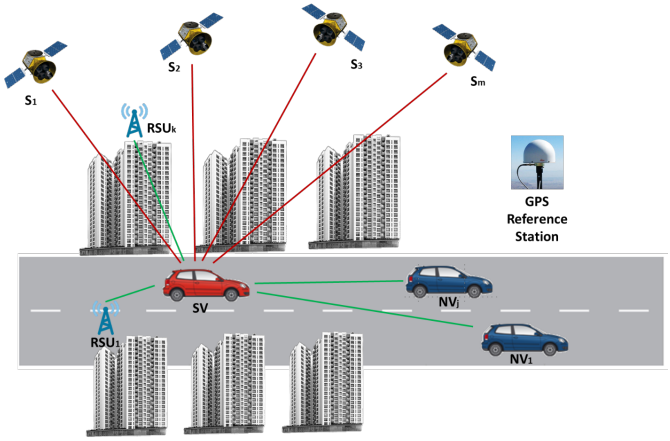

Fig. 1: System model of cooperative positioning

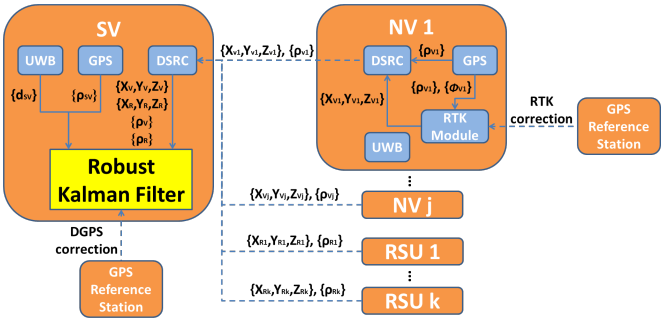

Fig. 2: The schematic of the proposed RCP method

$m > 5$). In addition, j neighbouring vehicles (NVs) and k RSUs are distributed in this road segment within the V2X communication range of SV. It is assumed that all nodes, including SV, NVs and RSUs, are equipped with a DSRC unit to establish the internode V2X connectivity as well as a UWB device to generate internode ranging measurement as drawn in green line in the figure. The SV is defined as a vehicle that knows its own GPS pseudo-range measurements, UWB ranging measurements, DGPS corrections from GPS reference station, and GPS pseudo-range measurements and accurate position of NVs and RSUs through DSRC. The NVs are defined as vehicles that are equipped with dual-frequency GPS receivers that can provide centimetre-level accuracy RTK positioning solutions. All RSUs are assumed to be located on pre-measured known positions which are shared to the SV through DSRC.

B. Robust Cooperative Positioning

The problem that is being addressed here is the development of a CP scheme to improve the positioning performance of the SV by fusing the available data from NVs and RSUs, especially in the case of urban canyon environment. Figure 2 shows the logical schematic of the proposed RCP method. In this approach, The NVs compute their positions from its on-board RTK module by receiving RTK corrections from GPS reference stations and then share their GPS pseudo-range measurements $\{\rho_V\}$ and computed positions $\{X_V, Y_V, Z_V\}$ with the SV. Besides, the RSUs shares their pre-measured accurate positions $\{X_R, Y_R, Z_R\}$ with the SV. On the SV's side, the UWB unit measures the internode ranging $\{d_{SV}\}$ between the SV and NVs or RSUs. In the meantime, the GPS receiver observes GPS pseudo-range measurements $\{\rho_{SV}\}$ and receives DGPS corrections from GPS reference stations. For data fusion, RKF is employed in this paper due to its advantages in handling outlier measurements compared to the Extended Kalman Filter (EKF). In RKF, a robust estimation based on the equivalent weight of the measurements is used to mitigate the outlier measurement influences.

For the construction of RKF in the proposed RCP method, the state vector $\hat{x}$ that contains the position $(\Delta x, \Delta y, \Delta z)$ and velocity $(\Delta\dot{x}, \Delta\dot{y}, \Delta\dot{z})$ of the SV and observation vector z that contains DGPS pseudo-range ρ_{m-1}^{DGPS} and UWB ranging measurements d_n^{UWB} of the SV are defined as:

$$\hat{x} = [\Delta x \quad \Delta\dot{x} \quad \Delta y \quad \Delta\dot{y} \quad \Delta z \quad \Delta\dot{z}]^T \tag{1}$$

$$z = [\Delta\rho_1^{DGPS}\Delta\rho_2^{DGPS}...\Delta\rho_{m-1}^{DGPS}\Delta d_1^{UWB}\Delta d_2^{UWB}...\Delta d_n^{UWB}]^T \quad (2)$$

Where m and n denote the numbers of visible GPS satellite and UWB units.

Well known DGPS measurement models can be found in [40]. The UWB system discussed in this paper uses Time Difference of Arrival (TDoA) ranging technique for positioning. TDoA technique is a variant of Time of Arrival (ToA) technique. TDoA is based on measuring the time difference between when signals arrive at different reference nodes, whereas ToA determines the time of flight of the signal, then derives the distance between the nodes. The merit of TDoA in comparison with ToA is that only the synchronisation among the reference receivers is required and there is no need for the transmission time at the object [41], [42]. UWB ranging measurement between unit a and unit n is defined as:

$$d_a^n = \sqrt{(X_a - X^n)^2 + (Y_a - Y^n)^2 + (Z_a - Z^n)^2} \quad (3)$$

The robust estimation of the state vector in the RKF can be reached through the prediction and update phases. The prediction phase represents the system's evolution from the previous to the current epoch. The new state vector $\hat{x}_{t+1|t}$ and associated covariance matrix $P_{t+1|t}$ are predicted from the state at epoch t to the state at epoch $t+1$ based on the dynamic model:

$$\hat{x}_{t+1|t} = F_{t+1}\hat{x}_{t|t} \quad (4)$$

$$P_{t+1|t} = F_{t+1}P_{t|t}F_{t+1}^T + Q_{t+1} \quad (5)$$

Where F_{t+1} is the state transition matrix which is applied to the previous state. Q_{t+1} is the associated process noise covariance matrix.

In the update phase, the posteriori state estimation and covariance matrix are updated by combining the current measurements and the priori predictions. Specifically, the robust estimation of the posterior state and corresponding covariance matrix then become:

$$\hat{x}_{t+1|t+1} = \hat{x}_{t+1|t} + \bar{K}_{t+1}V_{t+1} \quad (6)$$

$$V_{t+1} = z_{t+1} - H_{t+1}\hat{x}_{t+1|t} \quad (7)$$

$$P_{t+1|t+1} = P_{t+1|t} - \bar{K}_{t+1}H_{t+1}P_{t+1|t} \quad (8)$$

Where z_{t+1} is the input measurement at epoch $t+1$. H_{t+1} is the design matrix. V_{t+1} is the innovation vector. $\bar{K}_{t+1}$ is the Kalman gain that indicates how much the measurements contained in the innovation vector could influence the final state vector estimate, specifying:

$$\bar{K}_{t+1} = P_{t+1|t}H_{t+1}^T(H_{t+1}P_{t+1|t}H_{t+1}^T + \bar{R}_{t+1})^{-1} \quad (9)$$

In which $\bar{R}_{t+1}$ is the covariance matrix of the measurement noise at epoch $t+1$.

The equivalent weight matrix $\bar{W}$ is the reciprocal of $\bar{R}$ and is a diagonal matrix that consists of $\bar{w}_i (i = 1, 2, ..., n)$, where n is the number of measurements. Based on the method presented in [43], the equivalent weight of individual measurement $\bar{w}_i$ is defined as follows:

$$\bar{w}_i = \begin{cases} w_i & |V_i'| \le c_0 \\ w_i \cdot \frac{c_0}{|V_i'|} & c_0 < |V_i'| \le c_1 \\ \frac{w_i}{10000} & |V_i'| \ge c_1 \end{cases} \quad (10)$$

Where $V_i' = \frac{V_i}{\sigma_i}$ is the standardised residual corresponding to V_i' and $\sigma_i = \sqrt{R_{i,i}}$. c_0 and c_1 are two constants that are set to mitigate the contribution of the outlier measurements to the state estimator.

c_0 is normally chosen between 1.0 and 1.5 based on experience. However, 3.0 is applied in the proposed RCP method. The reason that we chose a value for c_0 exceeding the range is that the method in [43] applies to the single type of observation, i.e., GPS, while our method is dealing with mixed DGPS pseudo-range and UWB ranging measurements. As the measurement noise of DGPS pseudo-range is bigger than that of UWB ranging, the standardised residual of UWB ranging is more sensitive to magnify which leads to the over-screening of UWB ranging measurement. To this end, a bigger c_0 is chosen to retain more effective measurements.

In addition to the method presented in [43], an additional threshold c_1 (chosen as 10.0 in this paper) is added to the equivalent weight function to further mitigate the influence of outliers, especially the UWB outlier measurements. This is because the weight of individual measurement is scaled according to the innovation vector that is effectively the difference between the observation and predicted estimate. In the case of GPS outlier, the magnitude of GPS outlier is much smaller than that of GPS pseudo-range, thus, it rarely generates an extreme value to the innovation vector. Contrastingly, a UWB ranging outlier has a relatively larger magnitude comparing to the distance between the transmitter and the transducer. This often results in a spike value in the innovation vector that could reduce the effectiveness of the weight function. Therefore, this additional threshold is assigned to increase the robustness of the weight function against the outlier measurement. Note that the equivalent weight is not designed to be infinity when V_i' is larger than c_1 . That is because the number of visible satellites is less in urban areas compared with the open sky environment. An infinity equivalent weight leads to excluding an individual measurement, which may result in a shortage of measurement in computing position.

Overall, $\bar{w}_i$ is a descending function with respect to the standardised residual. When V_i' is less than c_0, the equivalent weight stays the same; the equivalent weight is divided by 10000 if V_i' is larger than c_1; and the equivalent weight is linearly reducing when V_i' is between c_0 and c_1.

IV. Performance Evaluations

The first part of this section presents the field experiment conducted to evaluate the performance of the proposed RCP method. The evaluations are extended in Section IV-B to simulated dataset, which are generated based on the collected field experiment dataset. More specifically, a GPS partial obstructed environment is simulated and four scenarios are considered for further performance assessment.

(a) (b)

Fig. 3: The GPS reference station and bundled UWB unit and GPS device

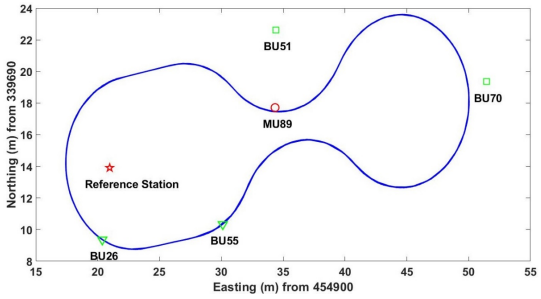

Fig. 4: Field experiment deployment

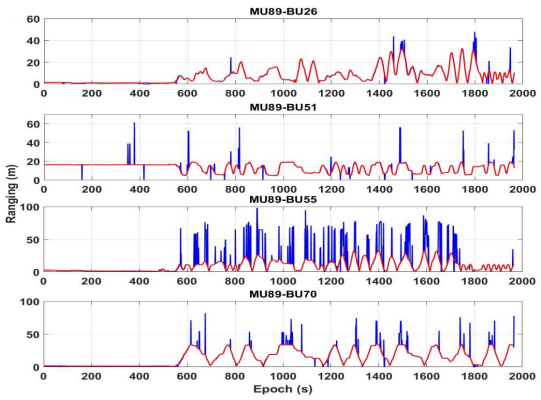

Fig. 5: Comparison between UWB raw ranging (blue) and ground truth distances (red)

A. Field experiment

A field experiment was conducted to evaluate the RCP method described above. Specifically, the setup introduces how the system model is implemented in practice. This is followed by the data analysis of raw UWB ranging measurements and a performance assessment of the RCP method.

1) Field experiment setup

The experiment was conducted on the roof of the Nottingham Geospatial Building (NGB) at the University of Nottingham, which consisted of a GPS reference station, three Leica dual-frequency GNSS receivers (GS10) that support RTK solutions and five UWB units. The UWB system used in the trials discussed throughout this thesis is the Thales UWB system which utilises a combination of Frequency Hopping and Direct Sequence Spread Spectrum signal covering 4760MHz to 6200MHz with output power level of -41.3dBm/MHz. The GPS reference station was located on a pillar on the roof of the NGB (See Figure 3a) to broadcast GPS corrections. The five UWB units included one Mobile Unit (MU), two moving Base Units (BUs) and two static BUs. Particularly, the two static BUs (BU51 and BU70) were located on a pillar and the edge of the roof respectively as shown in Figure 4, their coordinates were pre-surveyed by a Leica Robotic Total Station (TS30) to millimetre accuracy. The remaining three UWB units were individually tied together with a Leica GS10 receiver (as shown in Figure 3b). The moving BUs (BU26 and BU55) were tied to receivers GPS02 and GPS04 respectively to produce accurate positions from RTK. MU89 was set to record all UWB ranging measurements and attached with GPS07. The pseudo-range measurements of GPS07 were processed using the RCP method for positioning and the RTK solution was used to provide the reference ground truth. The three MU sets were carried by two people and a locomotive to move along the bell-shaped test track. An overview of the system deployment is displayed in Figure 4. According to the introduced system model in Section III-A, MU89 acts as the SV; BU26 and BU55 represent NVs; BU51 and BU70 represent RSUs.

The experiment started with 10 minutes of static data collection and followed by approximately 20 minutes of kinematic data collection, giving a total time of around 30 minutes. The UWB measurements were time-stamped with GPS time and collected at 1 Hz sampling rate. The sampling rate of GPS receivers was also configured to 1 Hz to match the UWB data rate. The proposed RCP method was used to post-process the collected data. However, as positions are generated iteratively per epoch, it is also suitable for real-time implementation.

2) Raw UWB ranging measurement assessment

Figure 5 shows the UWB ranging (in blue) compared to the ground truth (in red) derived from accurate GPS coordinates. This illustrate that the overall high accuracy of UWB ranging measurements, which can be contaminated by outliers occasionally. Particularly, the measurements of BU55 contained much more outliers compared to BU26, BU51 and BU70 .

Table I lists the detailed statistics of the UWB ranging performance for the field experiment. For all four ranging measurements, the availability remains higher than 97.8%. Here, an error larger than 4m is deemed as an outlier. As such, BU26 and BU51 had less than 2% outliers and BU55 had the highest outliers of 10.0%, which is due to that the unit being carried by a person which may cause disturbances. The outlier observed by the static BU70 was almost double the amount of BU51. This may be due to that BU70 was located at the end of the track with a smaller angle of view between the moving units and itself, therefore a higher possibility of NLOS disruptions. It can be noted that a better distribution of static BUs helps to reduce the occurrence of outliers. Overall, the UWB units provided a ranging accuracy of better than 40 cm regardless of the outliers.

TABLE I: UWB ranging evaluation (outlier excluded)

Total epoch (1965s)	**BU26**	**BU51**	**BU55**	**BU70**
Received observation	1921	1956	1949	1936
Availability (%)	97.8	99.5	99.2	98.5
Number of outlier	15	33	194	61
Outlier percentage (%)	0.8	1.7	10.0	3.2
RMS (cm) (Outlier excluded)	28.6	26.1	39.2	37.1
STD (cm) (Outlier excluded)	28.3	26.1	39.3	32.2

TABLE II: Positioning performance based on UWB ranging (EKF vs. RKF)

Time	**Method**		**E**	**N**	**H**	**2D**	**3D**
Static (before epoch 550)	EKF	RMS(m)	1.80	0.54	2.21	1.88	2.90
		STD(m)	1.78	0.50	2.20	1.82	2.81
		Max(m)	31.83	6.62	7.98	32.51	53.97
	RKF	RMS(m)	0.11	0.26	0.37	0.29	0.46
		STD(m)	0.07	0.15	0.18	0.12	0.17
		Max(m)	0.66	0.98	1.13	1.00	1.15
Kinematic (before epoch 550)	EKF	RMS(m)	9.50	9.67	13.28	13.56	18.97
		STD(m)	9.50	9.57	13.27	11.82	16.32
		Max(m)	126.38	79.15	176.45	130.28	219.33
	RKF	RMS(m)	0.33	0.67	1.53	0.75	1.70
		STD(m)	0.32	0.66	1.53	0.64	1.33
		Max(m)	1.66	8.36	12.51	8.37	14.92

3) Performance evaluation based on raw UWB measurement

As four groups of UWB ranging measurements were collected, the position of the SV can be solved based on UWB measurements alone. Table II lists the UWB standalone positioning performance comparison between applying the EKF method and the RCP method. E, N and H indicate the easting, northing and height coordinates respectively. Results are split into the static and the kinematic periods. It can be observed that the outliers can lead to significant degradation in positioning accuracy. In particular, the 2D and 3D static accuracies obtained through the KF method are 1.88m and 2.90m respectively while the kinematic accuracy degrades to worse than 10 metres. Moreover, the static and kinematic maximum position errors reach a few tens of metres and larger than a hundred metres respectively. In contrast, static and kinematic accuracies are significantly improved to the sub-metre level by applying the proposed RCP method. Specifically, the overall static and kinematic accuracies can achieve 0.29m and 0.75m in 2D and 0.46m and 1.70m in 3D respectively. Furthermore, the maximal position error has been limited within approximately 1 metre and 10 metres in the static and kinematic periods respectively. The decreased static and kinematic precisions of 0.12m and 0.64m in 2D and 0.17m and 1.33m in 3D also suggested improved reliability.

4) Performance evaluation based on raw DGPS/UWB measurements

The performance of the proposed RCP method is evaluated by comparing the positions in three directions computed based on sole DGPS and the integration of DGPS and UWB as shown in Figure 6 and Figure 7, which show the result of the static period (before epoch 550) and kinematic period (after epoch 550) respectively. The position error of the DGPS-standalone solution changes smoothly according to the

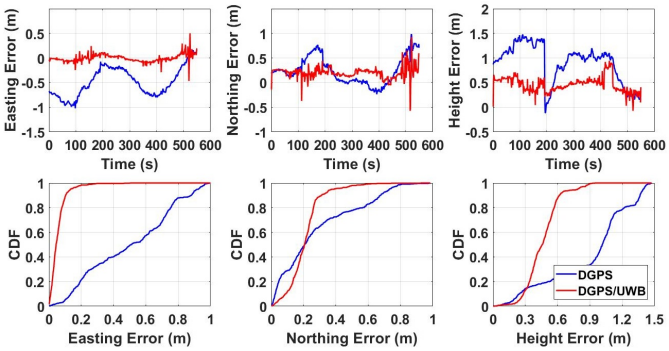

Fig. 6: Static position error comparison between DGPS-alone and integration of DGPS/UWB solutions using RCP method

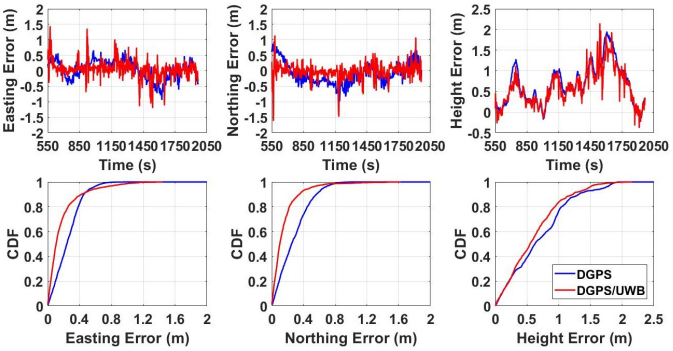

Fig. 7: Kinematic position error comparison between DGPS-alone and integration of DGPS/UWB solutions using RCP method

change of satellite geometry whereas the position error of DGPS/UWB case contains a number of spikes due to the UWB ranging outliers and sudden change of UWB unit geometry. Specifically, the spikes in easting and northing around epoch 550 occurred when MU89 started to move. The spikes in easting at around epoch 900 and in northing close to epoch 1200 are due to MU89 changing direction.

It can be concluded that relatively large errors often occur when the direction of motion changes suddenly. The large errors introduced from extra observations is due to the enlarged measurement noise covariance matrix R from the outliers (referring to Eq.4). The Kalman gain K is then decreased to reduce the weight of the estimated measurement model. Meanwhile, the estimate of the state model becomes inaccurate due to the sudden change in the motion direction. Therefore, the final position estimate of the RCP method inclines to the estimate of the state model which results in more spikes. It can be found that the errors of both cases stay within 2m and the Cumulative Distribution Function (CDF) figures depict that the employment of UWB observations can overall reduce the three directional position errors despite some accuracy compromises during the intervals containing outliers.

The statistical details of the positioning performance comparison between the DGPS standalone solution and DGPS/UWB combination are shown in Table III. The static DGPS-standalone case gives 0.68m accuracy and 0.22m precision in 2D and around 1.00m accuracy with a 0.40m precision

in height. By adding UWB measurements, the improvement of the static case is better than that of the kinematic case when compared to the DGPS standalone solution, as the static UWB ranging accuracy is much more accurate than that of DGPS pseudo-ranges with very few outliers. The static easting, northing and height accuracies are 0.08m, 0.23m and 0.48m with 86.3%, 36.6% and 51.0% improvements respectively by adding UWB ranging. In the kinematic case, the easting, northing and height accuracies of the combination case are 0.28m, 0.24m and 0.74m respectively with an approximately 10% improvement in easting and height directions and a 31.3% improvement in northing direction. Based on seven DGPS pseudo-range and four UWB ranging, the proposed RCP method can overall offer 0.25m 2D static accuracy and 0.54m 3D static accuracy as well as 0.36m 2D kinematic accuracy and 0.82m 3D kinematic accuracy after eliminating the severe UWB ranging outliers.

TABLE III: Positioning performance comparison between DGPS-alone and integration of DGPS/UWB solution using RCP method

Time	Case		E	N	H	2D	3D
Static (before epoch 550)	DGPS	RMS(m)	0.57	0.37	0.99	0.68	1.19
		STD(m)	0.30	0.28	0.39	0.22	0.35
		Max(m)	1.02	0.99	1.47	1.07	1.79
	DGPS/ UWB	RMS(m)	0.08	0.23	0.48	0.25	0.54
		STD(m)	0.08	0.12	0.15	0.11	0.14
		Max(m)	0.50	0.93	0.95	0.94	0.97
Accuracy improvement (%)			86.3	36.6	51.0	63.4	54.6
Kinematic (before epoch 550)	DGPS	RMS(m)	0.30	0.34	0.84	0.46	0.95
		STD(m)	0.30	0.33	0.49	0.21	0.40
		Max(m)	0.94	0.99	1.94	1.07	2.14
	DGPS/ UWB	RMS(m)	0.28	0.24	0.74	0.36	0.82
		STD(m)	0.27	0.24	0.44	0.26	0.41
		Max(m)	1.44	1.62	2.15	1.91	2.46
Accuracy improvement (%)			8.0	31.3	11.8	20.4	13.7

B. Simulation-based comprehensive performance analysis

To further evaluate the performance of the RCP method, a simulation dataset is generated by combining the raw GPS observations collected in the field experiment and simulated UWB ranging measurements. In addition, a GPS partially obstructed environment is also simulated and described in the following sub-sections. Four scenarios are considered based on the simulated GPS partially obstructed environment with the simulated dataset to comprehensively assess the positioning performance of the proposed RCP method.

1) Simulation setup

Although the effect of severe UWB measurement outliers have been significantly mitigated by the RCP method, the full potentials of additional measurement were not effectively exploited due to the restriction of the experimental environment. As each moving platform could not provide the same level of dynamics, the outliers suffered by each UWB units varied significantly. For instance, measurement from MU89-BU55 (carried by people) contained a larger percentage of outlier observations compared to measurement from MU89-BU26 (carried by a locomotive). To conduct a fair and controlled quantitative analysis to evaluate the benefits of UWB ranging augmentation, a group of UWB measurements were simulated based on the error distribution of collected raw UWB measurements. This simulated data is then integrated with the real GPS pseudo-range measurements collected in the field experiment to be processed through the proposed RCP method. Since our study focuses on the CAV applications, only the kinematic scenario is considered, i.e. UWB measurements are simulated based on the measurements after epoch 550. To pre-process the raw UWB measurement, all the ranging errors larger than 1 metre are removed. The simulated measurements are generated based on the original error distribution of the remaining raw data. Overall, 1416 measurements are generated for each BU based on the error distribution of raw UWB data collected from the field experiment. As the sufficient number of the redundant GPS measurements would relieve the effect of multipath observations without using the robust estimation approach, a GPS partially obstructed environment (effectively 4 visible GPS satellites) is constructed, as shown in Figure 8, as the environmental baseline for the following evaluations.

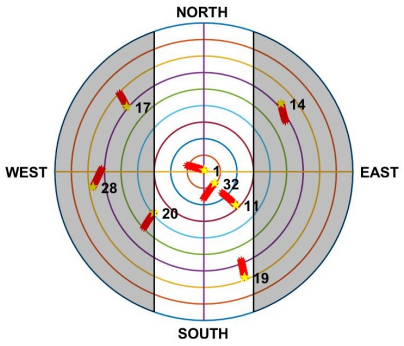

Fig. 8: The GPS sky plot of a north-south direction urban canyon with a 60 degrees cut-off angle (the red lines and yellow stars show the satellite trajectories and the ending position of the satellites respectively and the shadow indicate GPS obstruction)

According to the system model described in section III-A, various scenarios are designed to comprehensively evaluate the proposed RCP method. All scenarios are based on the defined urban canyon environment shown in Figure 8, the data applied are the collected GPS data in Section IV-A1 and the above mentioned simulated UWB ranging measurement. In total, four scenarios are discussed in the following sections:

- Scenario 1: Two sections of artificial GPS multipath error are introduced to assess the robustness of the proposed RCP method.
- Scenario 2: Different number of UWB measurements are integrated with DGPS to explore the benefits of additional UWB ranging.
- Scenario 3: Different number of DGPS measurements are integrated with UWB ranging to evaluate the effects of decreasing satellite number on the RCP positioning performance.
- Scenario 4: The Mobile Reference Station (MRS) concept is proposed as an alternative of the conventional Stationary Reference Station (SRS) to enable the DGPS solution.

2) Scenario 1

To assess the advantage of the proposed RCP method in presence of multipath, two sections of continuous GPS multipath varying between 25m and -25m are simulated during the epoch 50-250 and 850-1050 as shown on the top of Figure 13. The following three subfigures demonstrate the three directional position errors by using EKF (in blue) and RCP (in red). It can be found that the EKF position errors increased significantly during the periods with multipath, whereas this can be effectively constrained by the RCP method.

Table IV lists the positioning error comparison between EKF and RCP specifically of during the two periods with the multipath contamination under GPS partial obstruction. Due to the involvement of multipath, the positioning accuracies of using EKF are 1.44m and 0.82m in horizontal and larger than 3m in height respectively, while the maximal errors increase to 7m in horizontal and 10m in height. The utilisation of the RCP method improves the positioning accuracy to better than 30cm in horizontal and around 1m in height while the maximum errors are limited at less than 1m in horizontal and about 2m in height.

TABLE IV: Positioning performance under the GPS partial obstruction environment with the artificial GPS multipath and UWB ranging using standard EKF and RCP methods

Time(s)	Method		E	N	H	2D	3D
50 - 250	EKF	RMS(m)	0.62	1.30	3.56	1.44	3.84
		STD(m)	0.61	1.29	3.57	1.05	2.35
		Max(m)	2.78	7.22	10.22	7.32	12.08
	RKF	RMS(m)	0.15	0.22	0.82	0.27	0.77
		STD(m)	0.15	0.22	0.46	0.14	0.34
		Max(m)	0.45	0.76	1.78	0.81	1.93
Accuracy improvement (%)			75.8	83.1	77.0	81.3	79.9
850-1050	EKF	RMS(m)	0.56	0.61	3.31	0.82	3.41
		STD(m)	0.56	0.60	3.23	0.53	1.98
		Max(m)	2.02	2.40	8.46	2.68	8.68
	RKF	RMS(m)	0.15	0.19	1.29	0.24	1.32
		STD(m)	0.15	0.19	0.42	0.13	0.42
		Max(m)	0.57	0.64	2.57	0.66	2.58
Accuracy improvement (%)			73.2	68.9	61.0	70.7	61.3

3) Scenario 2

Assuming the SV is driven through the urban canyon depicted in Figure 8 between epoch 200 and epoch 400. Figure

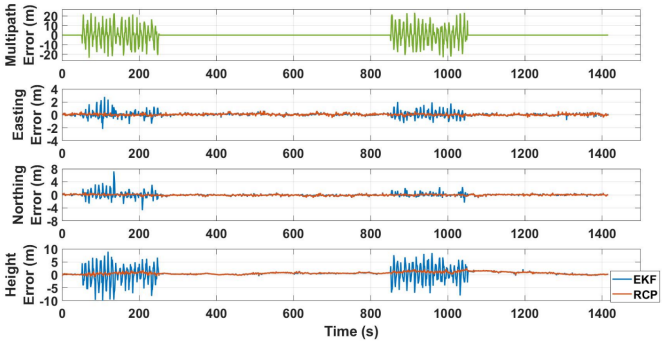

Fig. 9: Position error under the GPS partial obstruction environment with the artificial GPS multipath and UWB ranging using standard EKF and RCP methods

10 illustrates the position error comparison between using and not using UWB observation under the GPS partial obstruction situation. The blue and red lines indicate the positioning error based on DGPS-standalone and DGPS/UWB integrated results respectively. It can be seen that there is a clear drift in all three directions between epoch 200 and 400 when the SV is driven into the urban canyon. With the augmentation of UWB observations, the easting and northing position accuracies can maintain the same level while satellites are partially blocked, whereas the height position accuracy slightly fluctuates within a 2m range.

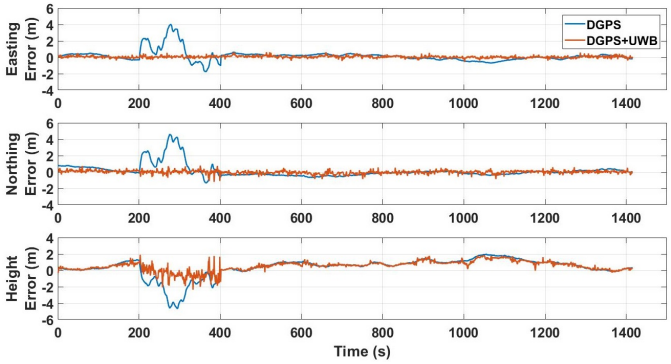

Fig. 10: Position error under the GPS partial obstruction (with UWB vs. without UWB)

To evaluate the potential improvement in positioning performance by integrating different numbers of UWB measurement, the position error CDF in three directions are drawn in Figure 11. The colour code indicates the different number of UWB ranging that is augmented in producing the SV's position. Specifically, the cyan line denotes the position error based on DGPS standalone solution with no redundant observations while the red line represents the positioning result based on three DGPS pseudo-ranges and four UWB ranging. It can be found that the introduction of UWB ranging could effectively improve the position accuracies in all three directions.

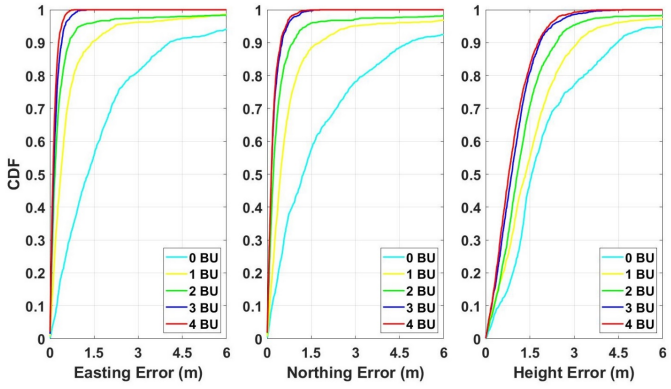

Fig. 11: Position error CDF using different numbers of simulated UWB ranging with three DGPS pseudo-range measurements

Table V lists the detailed results based on the number of additional UWB measurements. The DGPS-standalone solution provides 2.70m and 3.21m accuracies in easting and northing

directions, 3.06m in height. It is noted that there are two stages of significant improvements in accuracy. Firstly, there is a more than 40% improvement in horizontal accuracy and 26% of improvement in height accuracy by adding the first UWB ranging. The second significant improvement benefits by integrating three UWB ranging which leads to 90% and 60% improvements in horizontal and height accuracy respectively. Introducing all available UWB ranging, the accuracies can achieve 0.19m, 0.29m and 1.11m in easting, northing and height directions respectively and the precisions reach to a similar level. This results in a more than 90% accuracy improvement in horizontal and an approximately 80% accuracy improvement in 3D.

TABLE V: Positioning performance comparison using different numbers of simulated UWB ranging with three DGPS pseudo-range

Number of UWB ranging		E	N	H	2D	3D
0	RMS(m)	2.70	3.21	3.06	4.20	5.20
	STD(m)	2.50	2.79	2.72	3.07	3.53
1	RMS(m)	1.40	1.85	2.27	2.32	3.24
	STD(m)	1.39	1.75	2.21	1.98	2.40
Accuracy improvement (%)		48.4	42.3	26.0	44.8	37.6
2	RMS(m)	1.20	1.48	1.86	1.90	2.66
	STD(m)	1.19	1.43	1.86	1.76	2.12
Accuracy improvement (%)		55.6	54.0	39.1	54.7	48.7
3	RMS(m)	0.25	0.32	1.20	0.40	1.26
	STD(m)	0.25	0.32	1.18	0.26	0.67
Accuracy improvement (%)		90.9	90.0	60.8	90.4	75.7
4	RMS(m)	0.19	0.29	1.11	0.34	1.17
	STD(m)	0.18	0.29	1.08	0.21	0.63
Accuracy improvement (%)		93.2	91.0	63.6	91.8	77.6

4) Scenario 3

Assuming the SV is driving towards a tunnel with two RSUs and two NVs located behind, as the SV approaches the tunnel, the number of visible GPS satellites will drop until no GPS observation is available. To investigate the effect of the reducing number of the DGPS measurements on the positioning performance of the integrated DGPS/UWB solution, the position error CDF in three directions are illustrated in Figure 12. The colour code indicates the different number of DGPS pseudo-range that is involved in producing the position. For example, the red line indicates the position error based on three DGPS pseudo-ranges and four UWB ranging and blue line depicts the position error based on UWB-standalone solution. It can be noted that the positioning performance does not degrade significantly when the GPS satellites are all obstructed. This is due to the accurate ranging measurements offered by the UWB. Hence the ability to generate accurate positions with reduced observations. As the visible GPS satellites are distributed along the north-south direction in the urban canyon, the degradations in northing and height directions are larger than that of easting direction. As visible GPS satellites are distributed more widely in the north-south direction than east-west direction, the influence of the reduction of DGPS measurements in the northing and height accuracies could be more significant.

Table VI lists the numeric results of the positioning performance of four UWB ranging integrated with different number

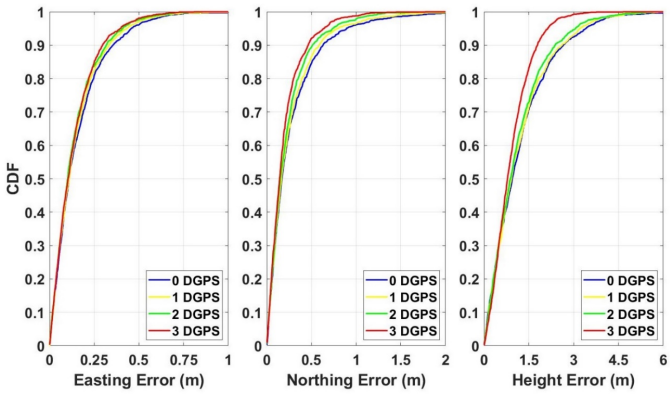

Fig. 12: Position error CDF using different number of DGPS pseudo-range measurements with four simulated UWB ranging

TABLE VI: Positioning performance comparison using different number of DGPS pseudo-range with four simulated UWB ranging

Number of DGPS code pseudorange		E	N	H	2D	3D
3	RMS(m)	0.19	0.29	1.11	0.34	1.17
	STD(m)	0.18	0.29	1.08	0.21	0.63
2	RMS(m)	0.19	0.34	1.46	0.39	1.51
	STD(m)	0.18	0.33	1.44	0.25	0.94
Accuracy degradation(%)		2.8	16.0	31.5	12.3	29.9
1	RMS(m)	0.21	0.39	1.55	0.44	1.61
	STD(m)	0.20	0.39	1.55	0.29	1.00
Accuracy degradation(%)		9.8	25.2	28.2	21.6	27.7
0	RMS(m)	0.22	0.43	1.61	0.48	1.68
	STD(m)	0.21	0.43	1.61	0.33	1.07
Accuracy degradation(%)		14.9	32.6	31.0	28.6	30.8

of DGPS measurements. It can be seen that no significant accuracy degradation is experienced when losing one DGP measurement. Moreover, the easting, northing and height accuracies fall by 9.8%, 25.2% and 28.2% respectively when only one DGPS pseudo-range measurement is available. When all satellites are obstructed, the positioning accuracy and precision worsen by 9cm in horizontal whereas there is a half metre degradation in height. In particular, the easting and northing accuracies drop by 2cm (14.9%), 14cm (32.6%) and 50cm (31.0%) respectively.

To investigate the impact of different network (including NVs and RSUs) geometry configuration on positioning improvement, the positioning errors and DOP values of GPS-only (in blue) case and UWB-only (in red) case in three directions are depicted in Figure 13. The GPS standalone case and UWB standalone case are based on four GPS pseudo-ranges and four UWB ranging measurements respectively. The top three figures show the errors whereas The bottom three figures reveal the Dilution of Precision (DOP) in easting, northing and height directions. respectively. DOP value is a indication of the geometric configuration of the GPS satellites or UWB BU where a smaller value means a good geometric configuration that may further result in a higher positioning accuracy. The definition and calculation of DOP value is

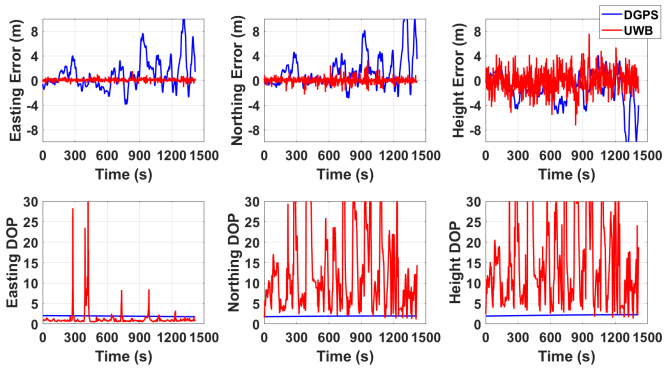

Fig. 13: The comparison of position error and DOP value between GPS-only and UWB-only cases

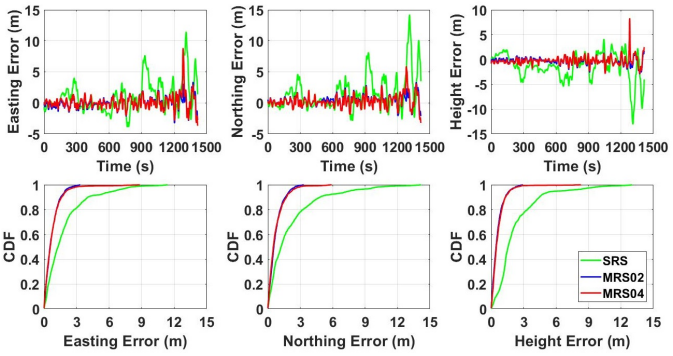

Fig. 14: Position error comparison based on DGPS-standalone solution using SRS and different MRSs

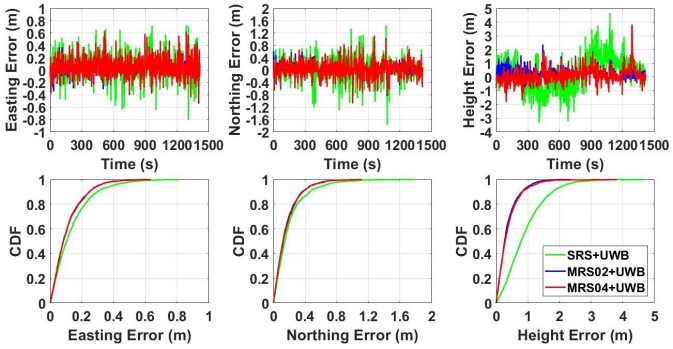

Fig. 15: Position error comparison based on DGPS/UWB integration solution using SRS and different MRSs

detailed in [44]. It can be seen that the positioning errors of UWB case outperform that of GPS case based on the same number of measurement, although the DOP values of GPS are much smaller than that of UWB's. In particular, the positioning errors of GPS case are 2.70m, 3.31m and 3.06m in easting, northing and height directions respectively, which can be found in V. In contrast, the positioning errors of UWB case are shown in VI, that are 0.22m, 0.43m and 1.61m correspondingly. For the DOP value comparison, GPS DOP values in three directions remain around 2, on the other hand, UWB DOP values are much worse. It is noted that the positioning errors of UWB case do not change accordingly when the corresponding DOP value becoming worse. In other words, there is no apparent correlation between UWB position error and DOP value.

5) Scenario 4

As common GPS multipath errors are spatially correlated within a small area, an NV close to the SV could provide better DGPS corrections than an SRS located further away. Based on the established V2X connectivity between the SV and an NV, the NV would act as an MRS and generate correction-like information, including the accurate coordinates based on RTK solution and raw GPS pseudo-range, which can be transmitted to the SV to enable the DGPS solution on the SV side.

Figure 14 and Figure 15 illustrate the position error and corresponding CDF of using SRS for DGPS-standalone solution and different MRSs (MRS02 and MRS04) that act as the MRS in the DGPS/UWB integration solution respectively, shown in green, blue and red lines respectively. The position error of the DGPS-standalone case using SRS corrections fluctuates within a 20m range, due to the limited number of visible satellite. With the utilisation of MRS, the three directional position errors are largely reduced. Specifically, the percentages of error within 3 metres in all three directions improve from 80% to almost 100%. This improvement is due to that the multipath errors observed by the SV and NV are highly correlated due to their close proximity, thus the DGPS correction technique can significantly reduce the errors on the SV. On the other hand, the employment of MRS does not introduce much improvement in the DGPS/UWB integration solution, due to the high accuracy in UWB measurements. The most significant improvement is seen in the height direction.

Table VII gives the statistics of the positioning performance using SRS, MRS02 and MRS04. Without the UWB observations, the SRS solution provides 2.70m easting accuracy, 3.21m northing accuracy and 3.06m height accuracy respectively. By contrast, the MRS02 and MRS04 solutions outperform the SRS solution by 68.0% and 61.7% in horizontal accuracy and 74.0% and 68.9% in height accuracy respectively. When four simulated UWB observations are used, the positioning accuracy of the SRS solution could achieve 0.19m, 0.29m and 1.11m in easting, northing and height directions respectively. The MRS solutions can further improve the horizontal accuracy by 20% and the height accuracy by more than 50%, which may be due to the similar height of MRS and the SV. Therefore a similar level of error is experienced from the external environment which can be better mitigated in the DGPS procedure. It is worth noting that the MRS02 solution always slightly outperforms the MRS04 solution, as the MRS04 was held by a person whereas the MRS02 was carried by the locomotive, which produces relatively stable movement and higher accuracy.

C. Discussions

Based on the assessments, the proposed RCP scheme demonstrates an improvement in positioning performance from three aspects: integration of UWB measurement, mitigating effect of the outlier measurements and implementation of the MRS-based DGPS solution.

TABLE VII: Positioning performance comparison using SRS and different MRSs

Case		E	N	H	2D	3D
SRS	RMS(m)	2.70	3.21	3.06	4.20	5.20
	STD(m)	2.50	2.19	2.72	3.07	3.53
MRS02	RMS(m)	0.95	0.95	0.80	1.34	1.56
	STD(m)	0.95	0.88	0.73	0.80	0.92
MRS04	RMS(m)	1.19	1.07	0.95	1.61	1.87
	STD(m)	1.19	1.04	0.92	1.15	1.30
Accuracy improvement(%)	MRS02	65.0	70.3	74.0	68.0	70.0
	MRS04	55.8	66.5	68.9	61.7	64.0
SRS+UWB	RMS(m)	0.19	0.29	1.11	0.34	1.17
	STD(m)	0.18	0.29	1.11	0.34	1.17
MRS02+UWB	RMS(m)	0.15	0.23	0.49	0.27	0.56
	STD(m)	0.14	0.22	0.43	0.16	0.33
MRS04+UWB	RMS(m)	0.15	0.23	0.55	0.27	0.62
	STD(m)	0.14	0.23	0.54	0.16	0.39
Accuracy improvement(%)	MRS02 + UWB	20.9	21.7	56.2	21.5	52.2
	MRS04 + UWB	19.5	20.3	50.6	20.1	47.2

Firstly, the augmented UWB ranging can significantly improve the positioning accuracy in GPS partially obstructed environment. However, the performance improvement from the integration of UWB ranging becomes limited in the open sky environment, as the GPS solution is able to provide a satisfactory accuracy with a sufficient number of visible satellites. It is also noted that the horizontal positioning accuracy based on four simulated UWB ranging measurements is as good as that of eight GPS pseudo-range measurements. In other words, using a large number of low accuracy measurements is less predominant in improving the performance than having less number of measurements but with high accuracy. This can be traced back to Section IV-B3 where the positioning accuracy improves from few-metres to decimetre-level by adding three UWB measurements; the positioning accuracy maintained at decimetre-level when all GPS measurements were lost in Section IV-B4. Furthermore, the comparison revealed in Figure 13 demonstrates that the degraded geometric configuration doesn't necessarily lead to a worse positioning accuracy as long as the accuracy ranging measurement remains good. Namely, the accuracy of ranging measurement is more predominant in improving the positioning performance than a better network geometry. In terms of outlier mitigation, the proposed RCP method proves to be effective in mitigating the influence of outlier measurements within the integrated positioning solution. this is demonstrated by the comparable results achieved in Section IV-A4, where real UWB data containing frequent outliers were processed by RCP, and Section IV-B3, where simulated UWB measurement with no outliers was applied. It also demonstrates that the RCP method is robust against the spiking outlier measurement as well as the continuous outlier measurement discussed in Section IV-B2. At last, the MRS-based solution outperforms that of conventional SRS solution in both with and without the integration of UWB measurement because the spatially correlated error is differenced out.

V. Conclusion

This paper proposed a novel cooperative positioning method, namely RCP, which integrates DGPS pseudo-range and UWB ranging measurement to provide a reliable and accurate position solution, enabled by V2X communication. The functionality and performance of the proposed method have been verified and evaluated by a real-world dataset and its extended simulation dataset. Besides, the UWB outlier ranging measurement problem was revealed and analysed to optimise thresholds of the robust estimation in RCP method. Analysis and experimental results in this paper showed that the proposed tight CP method could effectively mitigate the effects of outlier measurements and enhance the positioning performance especially in low GPS visibility and GPS outages, which is typical in dense urban areas and tunnels.

Due to the limitations of the experimental environment, the moving platform was restricted to a relatively low speed, which limits the realistic dynamics of the platform. Furthermore, actual V2X communication systems were not integrated within the solution. Therefore, the end-to-end delay and information exchange error due to mobility and channel variation in V2X communication cannot be examined. However, these limitations are been addressed in our future work. In addition, a weighted integration approach based on the quality of individual measurement deems to be a viable proposition that would warrant new investigations.

Acknowledgment

This work was supported in part by the Jaguar Land Rover and in part by the United Kingdom-Engineering and Physical Sciences Research Council (UK-EPSRC) as part of the jointly funded Towards Autonomy: Smart and Connected Control (TASCC) Programme under Grant EP/N01300X/1. This work is partially supported by Ningbo Science and Technology Bureau under Commonweal Research Program with project code 2019C50017 and a research grant with project code A0060 from Ningbo Nottingham New Material Institute.

References

[1] J. Barbaresso, G. Cordahi, D. Garcia, C. Hill, A. Jendzejec, K. Wright, and B. A. Hamilton, "Usdot's intelligent transportation systems (its) its strategic plan, 2015-2019." United States. Department of Transportation. Intelligent Transportation ..., Tech. Rep., 2014.

[2] C. Hancock, G. Roberts, and A. Taha, "Satellite mapping in cities: how good can it get?" in *Proceedings of the Institution of Civil Engineers-Civil Engineering*, vol. 162, no. 3. Thomas Telford Ltd, 2009, pp. 122–128.

[3] S. Ji, W. Chen, X. Ding, Y. Chen, C. Zhao, and C. Hu, "Potential benefits of gps/glonass/galileo integration in an urban canyon–hong kong," *The Journal of Navigation*, vol. 63, no. 4, pp. 681–693, 2010.

[4] P. D. Groves, "Shadow matching: A new gnss positioning technique for urban canyons," *Journal of Navigation*, vol. 64, no. 3, pp. 417–430, 2011.

[5] C. Hancock, P. Zhang, L. Lau, G. Roberts, and H. de Ligt, "Satellite mapping in cities and below cities: how good is it now?" in *Proceedings of the Institution of Civil Engineers-Civil Engineering*, vol. 170, no. 1. Thomas Telford Ltd, 2016, pp. 33–38.

[6] J.-P. Montillet, G. Roberts, C. Hancock, X. Meng, O. Ogundipe, and J. Barnes, "Deploying a locata network to enable precise positioning in urban canyons," *Journal of Geodesy*, vol. 83, no. 2, pp. 91–103, 2009.

[7] D. A. Grejner-Brzezinska, C. K. Toth, T. Moore, J. F. Raquet, M. M. Miller, and A. Kealy, "Multisensor navigation systems: A remedy for gnss vulnerabilities?" *Proceedings of the IEEE*, vol. 104, no. 6, pp. 1339–1353, 2016.

[8] S. Stephenson, X. Meng, T. Moore, A. Baxendale, and T. Edwards, "A fairy tale approach to cooperative vehicle positioning," 2014.

[9] J. Wang, Y. Gao, Z. Li, X. Meng, and C. M. Hancock, "A tightly-coupled gps/ins/uwb cooperative positioning sensors system supported by v2i communication," *Sensors*, vol. 16, no. 7, p. 944, 2016.

[10] Z. Li, R. Wang, J. Gao, and J. Wang, "An approach to improve the positioning performance of gps/ins/uwb integrated system with two-step filter," *Remote Sensing*, vol. 10, no. 1, p. 19, 2018.

[11] O. J. Woodman, "An introduction to inertial navigation," University of Cambridge, Computer Laboratory, Tech. Rep., 2007.

[12] R. Garello, J. Samson, M. A. Spirito, and H. Wymeersch, "Peer-to-peer cooperative positioning part ii: Hybrid devices with gnss & terrestrial ranging capability," *Inside GNSS*, pp. 20–29, 2012.

[13] N. Alam and A. G. Dempster, "Cooperative positioning for vehicular networks: Facts and future," *IEEE transactions on intelligent transportation systems*, vol. 14, no. 4, pp. 1708–1717, 2013.

[14] X. Meng, Y. Gao, H. Zhao, and J. Ryding, "Comprehensive assessment of uwb for indoor positioning and navigation," in *European Navigation Conference*, 2012, pp. 25–27.

[15] D. Wang, "Cooperative v2x relative navigation using tight-integration of dgps and v2x uwb range and simulated bearing," 2015.

[16] F. Shen, J. W. Cheong, and A. G. Dempster, "An ultra-wide bandwidth-based range/gps tight integration approach for relative positioning in vehicular ad hoc networks," *Measurement Science and Technology*, vol. 26, no. 4, p. 045003, 2015.

[17] A. R. J. Ruiz and F. S. Granja, "Comparing ubisense, bespoon, and decawave uwb location systems: Indoor performance analysis," *IEEE Transactions on instrumentation and Measurement*, vol. 66, no. 8, pp. 2106–2117, 2017.

[18] G. De Angelis, A. Moschitta, and P. Carbone, "Positioning techniques in indoor environments based on stochastic modeling of uwb round-trip-time measurements," *IEEE Transactions on Intelligent Transportation Systems*, vol. 17, no. 8, pp. 2272–2281, 2016.

[19] S. Marano, W. M. Gifford, H. Wymeersch, and M. Z. Win, "Nlos identification and mitigation for localization based on uwb experimental data," *IEEE Journal on selected areas in communications*, vol. 28, no. 7, pp. 1026–1035, 2010.

[20] K. Yu, K. Wen, Y. Li, S. Zhang, and K. Zhang, "A novel nlos mitigation algorithm for uwb localization in harsh indoor environments," *IEEE Transactions on Vehicular Technology*, vol. 68, no. 1, pp. 686–699, 2018.

[21] J. Gonzalez, J. Blanco, C. Galindo, A. Ortiz-de Galisteo, J. Fernández-Madrigal, F. Moreno, and J. Martinez, "Combination of uwb and gps for indoor-outdoor vehicle localization," in *2007 IEEE International Symposium on Intelligent Signal Processing*. IEEE, 2007, pp. 1–6.

[22] P. D. Groves, "Principles of gnss, inertial, and multisensor integrated navigation systems, [book review]," *IEEE Aerospace and Electronic Systems Magazine*, vol. 30, no. 2, pp. 26–27, 2015.

[23] G. MacGougan, K. O'Keefe, and D. S. Chiu, "Multiple uwb range assisted gps rtk in hostile environments," in *Proceedings of the 21st International Technical Meeting of the Satellite Division of The Institute of Navigation (ION GNSS 2008)*, 2008, pp. 3020–3035.

[24] G. D. MacGougan and R. Klukas, "Method and apparatus for high precision gnss/uwb surveying," in *Proceedings of the 22nd International Technical Meeting of The Satellite Division of the Institute of Navigation (ION GNSS 2009), Savannah, GA*. Citeseer, 2009, pp. 853–863.

[25] G. MacGougan, K. O'Keefe, and R. Klukas, "Tightly-coupled gps/uwb integration," *The Journal of Navigation*, vol. 63, no. 1, p. 1, 2010.

[26] Y. Jiang, M. Petovello, and K. O'Keefe, "Augmentation of carrier-phase dgps with uwb ranges for relative vehicle positioning," in *Proceedings of the 25th International Technical Meeting of The Satellite Division of the Institute of Navigation (ION GNSS 2012)*, 2012, pp. 1568–1579.

[27] J. N. Gross, Y. Gu, and M. B. Rhudy, "Robust uav relative navigation with dgps, ins, and peer-to-peer radio ranging," *IEEE Transactions on Automation Science and Engineering*, vol. 12, no. 3, pp. 935–944, 2015.

[28] K. Gryte, J. M. Hansen, T. Johansen, and T. I. Fossen, "Robust navigation of uav using inertial sensors aided by uwb and rtk gps," in *AIAA Guidance, Navigation, and Control Conference*, 2017, p. 1035.

[29] K. Liu, H. B. Lim, E. Frazzoli, H. Ji, and V. C. Lee, "Improving positioning accuracy using gps pseudorange measurements for cooperative vehicular localization," *IEEE Transactions on Vehicular Technology*, vol. 63, no. 6, pp. 2544–2556, 2013.

[30] N. Alam, A. T. Balaei, and A. G. Dempster, "A dsrc doppler-based cooperative positioning enhancement for vehicular networks with gps availability," *IEEE Transactions on Vehicular Technology*, vol. 60, no. 9, pp. 4462–4470, 2011.

[31] Y. Wang, X. Duan, D. Tian, M. Chen, and X. Zhang, "A dsrc-based vehicular positioning enhancement using a distributed multiple-model kalman filter," *IEEE Access*, vol. 4, pp. 8338–8350, 2016.

[32] E. Richter, M. Obst, R. Schubert, and G. Wanielik, "Cooperative relative localization using vehicle-to-vehicle communications," in *2009 12th International Conference on Information Fusion*. IEEE, 2009, pp. 126–131.

[33] H. Kloeden, D. Schwarz, E. M. Biebl, and R. H. Rasshofer, "Vehicle localization using cooperative rf-based landmarks," in *2011 IEEE Intelligent Vehicles Symposium (IV)*. IEEE, 2011, pp. 387–392.

[34] J. Roth, T. Schaich, and G. Trommer, "Cooperative gnss-based method for vehicle positioning," *Gyroscopy and Navigation*, vol. 3, no. 4, pp. 245–254, 2012.

[35] M. Elazab, A. Noureldin, and H. S. Hassanein, "Integrated cooperative localization for vehicular networks with partial gps access in urban canyons," *Vehicular Communications*, vol. 9, pp. 242–253, 2017.

[36] D. Wang, K. O'Keefe, and M. Petovello, "Decentralized cooperative navigation for vehicle-to-vehicle (v2v) applications using gps integrated with uwb range," in *Proceedings of the ION Pacific PNT 2013 Conference, Honolulu, HI, USA*, 2013, pp. 22–25.

[37] M. G. Petovello, K. O'Keefe, B. Chan, S. Spiller, C. Pedrosa, and C. Basnayake, "Demonstration of inter-vehicle uwb ranging to augment dgps for improved relative positioning," in *Proceedings of the 23rd International Technical Meeting of The Satellite Division of the Institute of Navigation (ION GNSS 2010)*, 2010, pp. 1198–1209.

[38] H. Ko, B. Kim, and S.-H. Kong, "Gnss multipath-resistant cooperative navigation in urban vehicular networks," *IEEE Transactions on Vehicular Technology*, vol. 64, no. 12, pp. 5450–5463, 2015.

[39] J. Xiong, J. W. Cheong, Z. Xiong, A. G. Dempster, S. Tian, and R. Wang, "Integrity for multi-sensor cooperative positioning," *IEEE Transactions on Intelligent Transportation Systems*, 2019.

[40] P. Misra and P. Enge, "Global positioning system: signals, measurements and performance second edition," *Global Positioning System: Signals, Measurements And Performance Second Editions*, vol. 206, 2006.

[41] B. O'Keefe, "Finding location with time of arrival and time difference of arrival techniques," *ECE Senior Capstone Project*, 2017.

[42] M. Ghavami, L. Michael, and R. Kohno, *Ultra wideband signals and systems in communication engineering*. John Wiley & Sons, 2007.

[43] Y. Yang, L. Song, and T. Xu, "Robust estimator for correlated observations based on bifactor equivalent weights," *Journal of geodesy*, vol. 76, no. 6, pp. 353–358, 2002.

[44] R. B. Langley *et al.*, "Dilution of precision," *GPS world*, vol. 10, no. 5, pp. 52–59, 1999.

Yang Gao Dr Yang Gao is currently working on the TASCC-CARMA as a Research Fellow in the Intelligent Vehicle Group at Warwick Manufacturing Group, the University of Warwick. He received his B.Sc. degree in Geographic Information System from China University Of Mining Technology, China in 2010, M.Sc. degree in Global Navigation Satellite System technology from the University of Nottingham, UK in 2011, and PhD at the University of Nottingham in 2017 on the topic of cooperative positioning for the V2X applications. His research interests include: cooperative positioning, multi-sensor integration and Connected and Autonomous Vehicles (CAVs).

Hao Jing Dr Hao Jing is currently a Senior Research Fellow in the Intelligent Vehicle Group at WMG, University of Warwick, with a research focus on high performance integrated and cooperative vehicle positioning and navigation solutions in challenging environments. Dr Jing previously completed her PhD at the University of Nottingham on the topic of collaborative indoor positioning. She has worked on a number of projects that focuses on achieving reliable and robust navigation performance for Connected and Autonomous Vehicles (CAV), pedestrians and mobile mapping systems in various environments and scenarios, based on solutions that make use of GNSS, LiDAR, IMU and wireless signals.

Mehrdad Dianati Professor Mehrdad Dianati leads Networked Intelligent Systems (Cooperative Autonomy) research at Warwick Manufacturing Group (WMG), University of Warwick. He has over 28 years of combined industrial and academic experience, with 20 years in leadership roles in multi-disciplinary collaborative RD projects, in close collaboration with the Automotive and ICT industries. He is also the Co-Director of Warwick's Centre for Doctoral Training on Future Mobility Technologies, training doctoral researchers in the areas of intelligent and electrified mobility systems in collaboration with the experts in the field of electrification from the Department of Engineering of the University of Warwick. In the past, he served as an associate editor for the IEEE Transactions on Vehicular Technology and several other international journals, including IET Communications. Currently, he is the Field Chief Editor of Frontiers in Future Transportation. His academic experience includes over 25 years of teaching undergraduate and post-graduate level courses and supervision of research students. He currently leads a post-graduate course in Machine Intelligence.

Craig Hancock Dr Craig Hancock is a Senior Lecturer in Surveying at Loughborough University. Formally Dr Hancock was an Associate Professor at the University of Nottingham Ningbo China. He has published over 80 research papers in subjects covering GNSS errors, Structural Health Monitoring and Navigation.

Xiaolin Meng Professor Xiaolin Meng is Fellow of the Royal Institute of Navigation and a member of its Technical Committee. He was Professor of Intelligent Mobility and Theme Leader of Positioning and Navigation Technologies at the University of Nottingham. His researches mainly focus on Intelligent Transportation Systems and Smart Cities, Connected and Autonomous Vehicles, Structural Health Monitoring of large infrastructure and Precision Agriculture/Livestock Farming, with an existing research portfolio of more than £18m. He led his international bridge monitoring team to win The Engineer Collaborate to Innovate Awards 2019 on digital innovation. He has made contributions to ESA, EU, UK, China on satellite-centred positioning and navigation, 5G and driverless vehicle policies. Professor Meng is an author of more 340 publications. He chaired major international associations' task forces and is a regular organiser and speaker in large international conferences. He is Associate Editor of Journal of Navigation, reviewer, guest editor-in-chief and board member of other world leading international journals. Professor Meng founded one and is mentoring two successful spinoff UK companies. As a CPD training organiser Professor Meng has led the Executive training courses to 286 Chinese CEOs and young academic leaders in the past 11 years. He is founding director of the Sino-UK Geospatial Engineering Centre – an international knowledge exchange centre in geospatial field. Professor Meng holds 7 guest professorships from top Chinese Universities and academies and currently working as Chair Professor of Smart Infrastructure in one of them.